⌘ *Author's Choice*

THE JOURNAL OF BIOLOGICAL CHEMISTRY VOL. 287, NO. 19, pp. 15896–15905, May 4, 2012

Six-transmembrane Topology for Golgi Anti-apoptotic Protein (GAAP) and Bax Inhibitor 1 (BI-1) Provides Model for the Transmembrane Bax Inhibitor-containing Motif (TMBIM) Family*[S]

Received for publication, December 21, 2011, and in revised form, February 28, 2012 Published, JBC Papers in Press, March 14, 2012, DOI 10.1074/jbc.M111.336149

Guia Carrara[‡§], **Nuno Saraiva**[‡§], **Caroline Gubser**[§1], **Benjamin F. Johnson**[§], **and Geoffrey L. Smith**[‡§2]

From the [‡]*Department of Pathology, University of Cambridge, Tennis Court Road, Cambridge CB2 1QP, United Kingdom and the* [§]*Section of Virology, Department of Medicine, Imperial College London, Norfolk Place, London W2 1PG, United Kingdom*

Background: Golgi anti-apoptotic protein (GAAP) is a regulator of intracellular Ca^{2+} fluxes and apoptosis.
Results: The transmembrane topology of viral GAAP is conserved in human GAAP and BI-1.
Conclusion: GAAPs and BI-1 have a six membrane-spanning topology with cytosolic N and C termini and a C-terminal reentrant loop.
Significance: The topology of the TMBIM family provides valuable structural information on these proteins.

The Golgi anti-apoptotic protein (GAAP) is a hydrophobic Golgi protein that regulates intracellular calcium fluxes and apoptosis. GAAP is highly conserved throughout eukaryotes and some strains of vaccinia virus (VACV) and camelpox virus. Based on sequence, phylogeny, and hydrophobicity, GAAPs were classified within the transmembrane Bax inhibitor-containing motif (TMBIM) family. TMBIM members are anti-apoptotic and were predicted to have seven-transmembrane domains (TMDs). However, topology prediction programs are inconsistent and predicted that GAAP and other TMBIM members have six or seven TMDs. To address this discrepancy, we mapped the transmembrane topology of viral (vGAAP) and human (hGAAP), as well as Bax inhibitor (BI-1). Data presented show a six-, not seven-, transmembrane topology for vGAAP with a putative reentrant loop at the C terminus and both termini located in the cytosol. We find that this topology is also conserved in hGAAP and BI-1. This places the charged C terminus in the cytosol, and mutation of these charged residues in hGAAP ablated its anti-apoptotic function. Given the highly conserved hydrophobicity profile within the TMBIM family and recent phylogenetic data indicating that a GAAP-like protein may have been the ancestral progenitor of a subset of the TMBIM family, we propose that this vGAAP topology may be used as a model for the remainder of the TMBIM family of proteins. The topology described provides valuable information on the structure and function of an important but poorly understood family of proteins.

The Golgi anti-apoptotic protein (GAAP)[3] was identified in camelpox virus as a highly hydrophobic protein that resides in the Golgi complex and regulates apoptosis (1). Highly conserved relatives of GAAP are present in three strains of vaccinia virus (VACV), the vaccine used to eradicate smallpox (2), and throughout eukaryotes including mammals, insects, fish, plants, yeast, and protozoa (1, 3). GAAPs are characterized by their very similar length, with the majority differing by only 1–4 amino acids in length, their high sequence similarity, and their highly conserved hydrophobicity profile (1). The GAAPs from VACV and camelpox virus (vGAAP) share 95% amino acid identity and are also very closely related to the human GAAP (hGAAP) which shares 73% amino acid identity with vGAAP (1). This degree of conservation is unusually high, and other poxvirus proteins that modulate innate immunity and are orthologues of cellular proteins are much more diverse. For instance, the VACV IFNγ receptor shares only ~20% amino acid identity to the IFNγ-binding extracellular region of its human IFNγ receptor (4, 5). The conservation of GAAPs extends throughout eukaryotes, and in some species gene duplication and diversification have occurred. For instance, in *Arabidopsis thaliana* there are five GAAPs, which share ~38% amino acid identity to hGAAP and have a very similar hydrophobicity profile (1).

Conservation among GAAPs is also evident at the functional level. Human GAAP is expressed in all tissue types and is essential for cell viability in tissue culture, but its loss can be complemented by vGAAP (1, 6). Furthermore, both vGAAP and hGAAP inhibit apoptosis induced by both intrinsic and extrinsic pro-apoptotic stimuli, such as Bax, staurosporine, doxorubicin, C_2-ceramide, Fas, and TNFα (1). More recently, it was reported that hGAAP lowers the amount of Ca^{2+} loaded in intracellular stores, thus reducing the amount of inositol 1,4,5-trisphosphate receptor-mediated Ca^{2+} released from these stores and rendering cells less sensitive to apoptotic stimuli (7).

* This work was supported by a grant from the Medical Research Council.
⌘ *Author's Choice*—Final version full access.
[S] This article contains supplemental Figs. 1–6.
[1] Present address: Developmental and Molecular Pathways, Novartis Institutes for BioMedical Research, 4056 Basel, Switzerland.
[2] Wellcome Trust Principal Research Fellow. To whom correspondence should be addressed. E-mail: gls37@cam.ac.uk.
[3] The abbreviations used are: GAAP, Golgi anti-apoptotic protein; BI-1, Bax inhibitor 1; CFP, cyan fluorescent protein; ER, endoplasmic reticulum; GalT, galactosyltransferase; hGAAP, human GAAP; Lfg, lifeguard; TMBIM, transmembrane Bax inhibitor-containing motif; TMD, transmembrane domain; VACV, vaccinia virus; vGAAP, viral GAAP.

However, the mechanism(s) by which these functions are mediated remain unknown, and it is unclear whether the ability of GAAP to regulate apoptosis relies on its Ca^{2+} regulatory function or whether these are two separate functions (1, 7).

GAAP is classified as the fourth member of the transmembrane Bax inhibitor containing motif (TMBIM) family. This family is characterized by conserved features such as a signature region from the beginning of the third to the middle of the fourth predicted transmembrane domain (TMD) (8), similar hydrophobicity profiles, and anti-apoptotic function (3, 9, 10). Members of this family include RECS1 (TMBIM1), FAIM2/Lfg (TMBIM2), GRINA (TMBIM3), GAAP (TMBIM4), Ghitm (TMBIM5), and BI-1 (TMBIM6) (1, 3, 10, 11). The most closely related family members to GAAPs are lifeguard (Lfg) and Bax inhibitor 1 (BI-1) with 34 and 28% amino acid identity, respectively (1). Like GAAP, BI-1 also protects cells against intrinsic pro-apoptotic stimuli (10, 12, 13) and lowers resting Ca^{2+} concentrations in the ER, which reduces Ca^{2+} release from intracellular stores upon stimulation, thus dampening the apoptotic response (14–16).

Bioinformatic analysis of the TMBIM family members found no known signal peptides or functional motifs (3). However, a series of charged residues at the C terminus of BI-1, EKDKKKEKK, which show some conservation in GAAPs, are important for its anti-apoptotic, cell adhesion, and calcium regulatory functions (13, 15, 17).

The highly conserved hydrophobicity profile of GAAPs and TMBIM members suggests that structure must be an important aspect of the function of these proteins. However, the literature and bioinformatics software are inconsistent about the overall topology of GAAP and BI-1, describing either a six- or seven-TMD profile (1, 3, 18), thus placing the N and C termini on the same or opposing sides of the membrane, respectively. Recently the N and C termini of BI-1 were reported to be in the cytosol (18, 19), but further experimental evidence of the topology of BI-1 or other TMBIM members is lacking. This prompted us to map the topology of vGAAP in detail. This mapping was based on the accessibility of antibody against strategically placed epitope tags following selective permeabilization of membranes. Data obtained demonstrate that vGAAP, hGAAP, and BI-1 have six TMDs with both the N and C termini in the cytosol and a putative reentrant loop at the C terminus. This topology is therefore likely to be conserved in other members of the TMBIM family. Furthermore, a series of charged residues at the C terminus of hGAAP were identified to be important for the inhibition of apoptosis triggered through a broad range of stimuli and therefore places these functionally important residues on the cytoplasmic side of Golgi membrane.

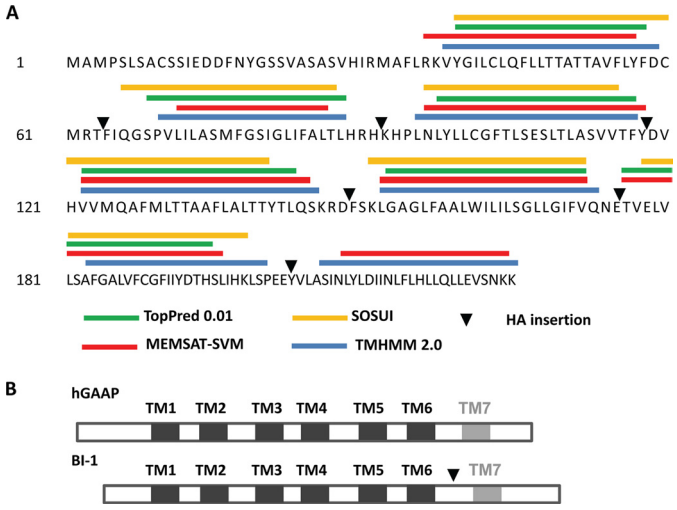

FIGURE 1. **Potential membrane topologies of members of the GAAP family.** *A*, amino acid sequence of VACV strain Evans GAAP and TMDs predicted by TMHMM 2.0 (*blue*), MEMSAT-SVM (*red*), TopPred 0.01(*green*) and SOSUI (*orange*). *B*, schematic illustration of hGAAP and BI-1 transmembrane regions (TM1–TM7) predicted by MEMSAT-SMV (*black*) and an additional transmembrane region predicted by MEMSAT3 (*gray*). Positions of individual HA tags insertions into VACV GAAP and BI-1 are indicated (*black triangles*).

EXPERIMENTAL PROCEDURES

Bioinformatics—TMD regions were predicted using algorithms TopPred 0.01, SOSUI, TMHMM 2.0, MEMSAT-SVM, and MEMSAT3. Multiple amino acid sequence alignments were generated using ClustalW 1.83.

Antibodies—The rabbit polyclonal GAAP antibody used for immunostaining is N terminus-specific (h- and v-GAAP residues 11–23 and 10–22, respectively, SSIEDDFNYGSSV) and was described previously (1). Antibodies and dilutions used for immunoblotting are as follows: rabbit anti-GFP (1:1,000; Abcam), which cross-reacts with derivatives of GFP, mouse anti-V5 (1:1,000; Serotec), rabbit anti-HA (1:10,000; Sigma), and mouse anti-calnexin (1:1,000; Transduction Laboratories).

Generation of Expression Plasmids and Stable Cell Lines—Full-length BI-1 was amplified by PCR and cloned into vector pECFP-1 (Clontech) using restriction sites XhoI/EcoRI to fuse CFP at the N terminus, or NheI/AgeI to fuse CFP at the C terminus of BI-1. Full-length vGAAP and hGAAP were amplified by PCR and cloned into vector pEYFP-C1 (Clontech) using restriction sites NheI/AgeI to fuse YFP at the C terminus of vGAAP and hGAAP. The QuikChange multisite-directed mutagenesis kit (Stratagene) was used to insert one HA epitope tag (YPYDVPDYA) per vGAAP-YFP plasmid at insertion sites TMD 1–2, 2–3, 4–5, and 6–7 (Fig. 1*A*). Two-step overlapping PCR was used to amplify full-length vGAAP or BI-1, incorporating an HA tag at sites TMD 3–4 or 5–6 for vGAAP, or TMD 6–7 for BI-1 (Fig. 1), and were cloned into the pEYFP-C1 vector (Clontech) using restriction sites NheI/AgeI. These series of plasmids were made to encode a flexible linker (GGSGGSGGSKR) introduced between GAAP or BI-1 and the fluorescent tag to allow folding flexibility. hGAAP with an N-terminal V5 tag was generated by PCR amplification of full-length hGAAP using a primer containing the V5 sequence and cloned into the MluI/BamHI site of the HIV-1-based lentivirus vector pdlNot'MCS'R'PK derived from pHR-SIN-CSGW (20). Full-length vGAAP and hGAAP with an HA tag at the C terminus were described (1). A region from TMD 6 to the C terminus of vGAAP (amino acids 203–237) including a HA tag at the C terminus was amplified using corresponding primers and ligated into pcDNA3.1 using restriction sites NheI/EcoRI to generate the truncation vGAAP TMD 7-HA. GalT-GFP and GRASP65-GFP were described (21).

Cell Culture and Transfection—HeLa cells were maintained in minimal essential medium supplemented with 10% fetal

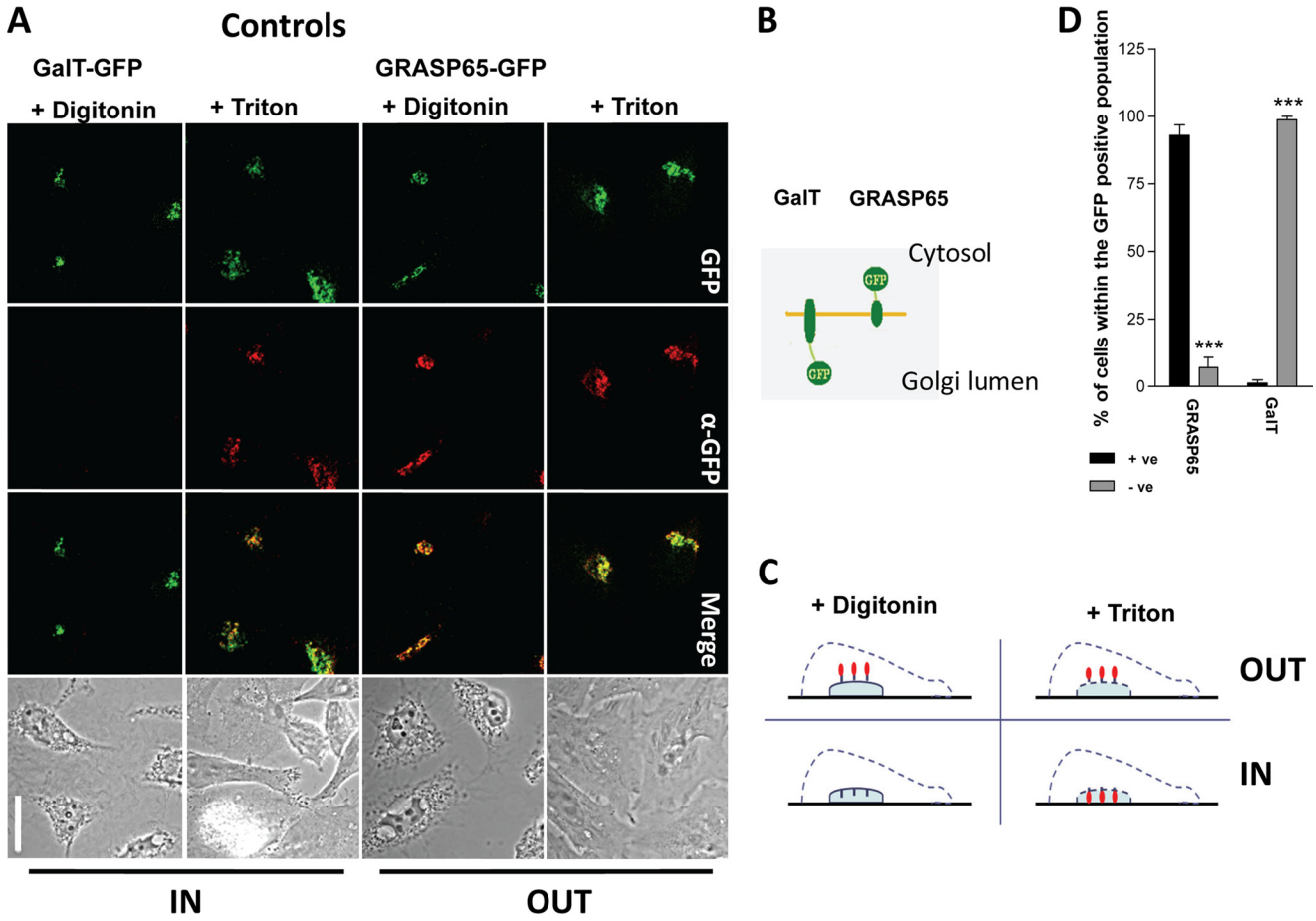

FIGURE 2. **Antibody probing of control proteins of known topology.** *A*, HeLa cells transfected with plasmids expressing control Golgi resident proteins of known topology, GalT-GFP, and GRASP65-GFP (21). The orientations of fluorescent tags were verified based on their accessibility with GFP antibody following complete or cell surface permeabilization with Triton X-100 or digitonin, respectively. *Scale bar*, 20 μm. *B*, schematic representation of GalT-GFP and GRASP65-GFP topology on the Golgi membrane. *C*, schematic representation of selective permeabilization assay used to determine the topology of epitopes based on their accessibility with corresponding antibody. Following treatment with 20 μM digitonin, only cytosolic-orientated epitope tags (*red*) are accessible and stained by antibody, whereas complete permeabilization with 0.1% Triton X-100 allows detection of epitope tags regardless of their orientation. *IN* and *OUT* refer to the epitope being located on the luminal or cytoplasmic side of organelle membranes, respectively. Conditions for digitonin treatment were optimized as described by Lorenz *et al.* (22). *D*, efficiency of digitonin treatment in topology assays addressed in cells expressing control alleles GRASP65-GFP and GalT-GFP. Data are presented as the mean (± S.E.; *error bars*) percentage of cells positive (*black*) or negative (*gray*) for GFP antibody staining within the transfected cell population. Each experiment was carried out in triplicate. Statistical analyses were carried out using unpaired Student's *t* test; ***, $p < 0.0005$.

bovine serum (FBS), penicillin, streptomycin, and 2 mM L-glutamine. Plasmid transfections were carried out using FuGENE (Roche Diagnostics) according to the manufacturer's instructions.

Immunofluorescence—Cells were grown on glass coverslips to a 70–80% confluence and transfected as above. After 16 h, cells were washed three times in KHM buffer (110 mM potassium acetate, 20 mM HEPES, 2 mM $MgCl_2$) at 4 °C. Cells were treated with either 0.1% Triton X-100 for 5 min to permeabilize all membranes or 20 μM digitonin (Sigma-Aldrich) in KHM buffer for 4 min at 4 °C to permeabilize the plasma membrane and were then washed twice with KHM buffer and incubated for 30 min in blocking buffer (0.2% gelatin in PBS) at 4 °C.

Conditions for digitonin treatment were optimized as described by Lorenz *et al.*, treating cells expressing free YFP with increasing digitonin concentrations (22). Effective permeabilization of the plasma membrane was established as the lowest digitonin concentration required for the loss of fluorescent signal in these cells as YFP diffuses freely in the cytosol and into the extracellular medium. Incubation with primary (1 h) and secondary antibody (30 min) was carried out sequentially in blocking buffer followed by washing three times with blocking buffer for a total of 30 min. Primary antibodies were used at a dilution of 1:50 N terminus-specific polyclonal rabbit anti-GAAP (1), 1:3,000 rabbit anti-GFP (Abcam), 1:1,000 mouse anti-V5 (Serotec), 1:200 mouse anti-HA (Sigma), and secondary antibodies conjugated to Alexa Fluor 488 or 568 (Invitrogen) were used at 1:500 dilution. Cells were fixed with 4% (w/v) paraformaldehyde at 4 °C for 20 min prior to permeabilization for completely permeabilized cells or after primary antibody incubation for selectively permeabilized cells. Coverslips were mounted onto slides using mounting medium (Moviol 4-88) containing 4′,6-diamidino-2-phenylindole (DAPI).

Stable Cell Lines—U2OS cell line neo and hGAAP were described (1), and hGAAP Cmut was generated in the same manner, using pCDNA3.1 encoding hGAAP in which charged amino acids, 234 and 236–8, have been mutated to alanine. Both hGAAP and hGAAP Cmut encode an HA epitope at the C terminus.

Apoptosis Assays—Neo, hGAAP, and hGAAP Cmut U2OS cell lines were seeded into 6-well dishes at $4-6 \times 10^5$ cells/well. The following day, cells were mock-treated or treated with 10 μg/ml cisplatin for 24 h, 3 μM doxorubicin in 2.5% FBS for 48 h, or 10 μg/ml cycloheximide (Sigma) alone or together with 500 ng/ml anti-human Fas antibody (Upstate Biotechnology) for 24 h. Both adhered and floating cells were harvested using 4 mM EDTA/PBS, and their DNA content was analyzed using flow cytometry. Statistical analysis was conducted using unpaired Student's *t* test on Prism 5.

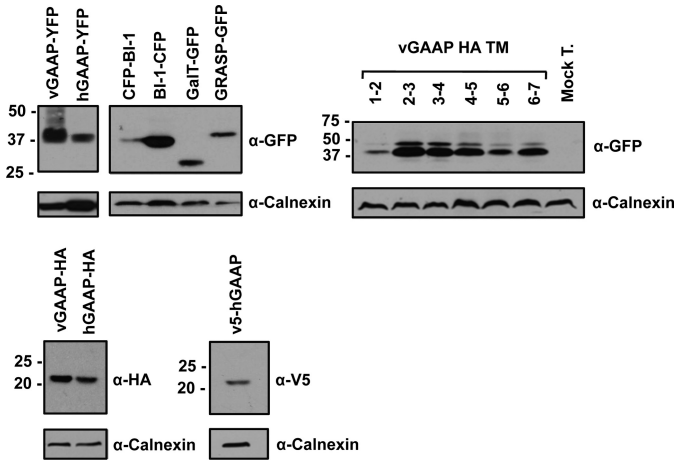

FIGURE 3. **Expression of alleles.** HeLa cells were either mock transfected (*Mock T*) or transfected with plasmids expressing different vGAAP, hGAAP, and BI-1 alleles or with plasmids expressing control proteins, GalT-GFP, and GRASP65-GFP, and cell extracts were prepared 16 h later and analyzed by immunoblotting. Allele V5-hGAAP was expressed and harvested from a HeLa cell line. The alleles tested were vGAAP-YFP, hGAAP-YFP, CFP-BI-1, BI-1-CFP, vGAAP-YFP containing a HA tag inserted between putative TMD 1–2, 2–3, 3–4, 4–5, 5–6, or 6–7, vGAAP-HA, hGAAP-HA, and V5-hGAAP.

RESULTS

Two Potential Topology Models for vGAAP and hGAAP, and Members of TMBIM Family—The membrane topology of vGAAP predicted by different algorithms TopPred 0.01 (23) or SOSUI (24), and TMHMM 2.0 (25) or MEMSAT-SVM (26) resulted in two differing topology profiles, one consisting of six TMDs and another composed of seven TMDs (Fig. 1*A*). All algorithms are consistent in predicting a cytoplasmic N terminus and the first six TMDs. However, they differed in the presence or absence of a seventh TMD, between residues 214 and 236 (Fig. 1*A*). This would therefore predict the C terminus to be located in the lumen or the cytosol, respectively. Similarly, two differing topology profiles were also predicted by algorithms MEMSAT-SVM (26) and MEMSAT3 (27) for hGAAP and BI-1, other TMBIM family members (Fig. 1*B*, *gray*). Like vGAAP, the N terminus of hGAAP and BI-1 was consistently predicted to be in the cytosol, but the C terminus could either be cytosolic or luminal depending on the number of predicted TMDs. This discrepancy required experimental investigation.

Validation of Epitope Accessibility Assay upon Selective Permeabilization—To investigate membrane topology, epitope tags were strategically placed at different hydrophilic regions within GAAPs and BI-1, and an epitope accessibility assay was employed to determine whether these epitopes were cytosolic or luminal. Cells were treated with 20 μM digitonin for 4 min, allowing the permeabilization of the plasma membrane only and keeping internal membranes such as the Golgi and the ER intact. Under these conditions, only cytosolic orientated epitopes are accessible and stained with antibody (Fig. 2*C*). However, complete permeabilization with 0.1% Triton X-100 for 5 min allowed detection of epitope tags regardless of their orientation on the membrane (Fig. 2*C*). Golgi resident proteins of known topology, GRASP65 and galactosyltransferase (GalT)

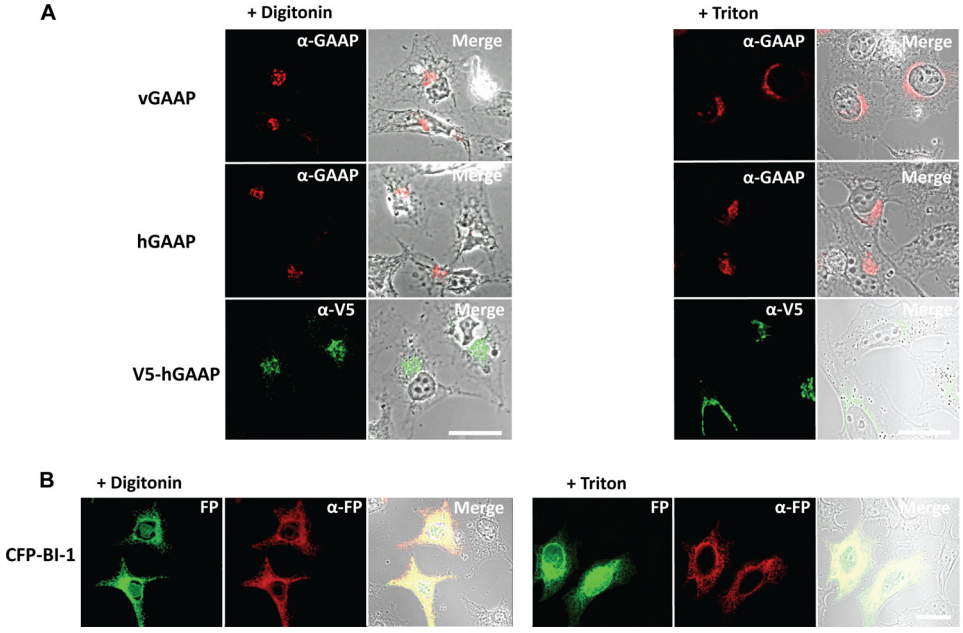

FIGURE 4. **N-terminal topology of members of the TMBIM family.** *A*, membranes of HeLa cells expressing vGAAP-HA, hGAAP-HA, and N-terminally V5-tagged hGAAP were selectively or completely permeabilized with digitonin (+ *Digitonin*) or Triton X-100 (+ *Triton*), respectively. The GAAP N terminus was probed using the N terminus-specific anti-GAAP antiserum (1), and the V5 tag was probed with anti-v5 antibody. *B*, fluorescent protein fused at the N terminus of BI-1 was probed with cross-reactive GFP antibody (α-*FP*) following selective or complete permeabilization with digitonin or Triton X-100, respectively. *Scale bar*, 20 μm.

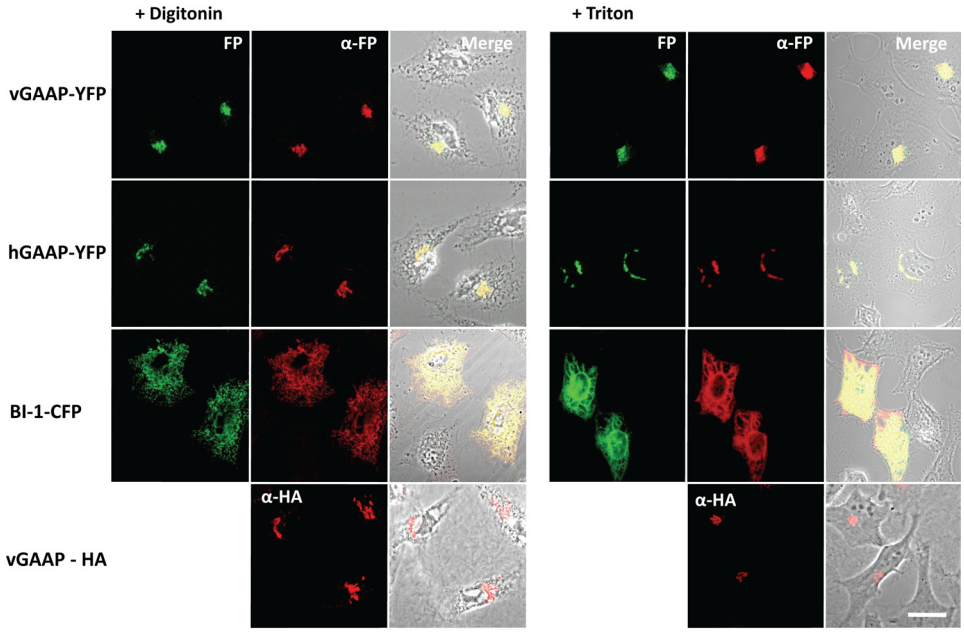

FIGURE 5. **C-terminal topology of members of the TMBIM family.** HeLa cells transfected with plasmids expressing vGAAP, hGAAP, or BI-1 fused at the C terminus with fluorescent or HA tags, were selectively or completely permeabilized with digitonin or Triton X-100, respectively. Tags were probed with antibody to fluorescent protein (*α-FP*) or to HA (*α-HA*). *Scale bar*, 20 μm.

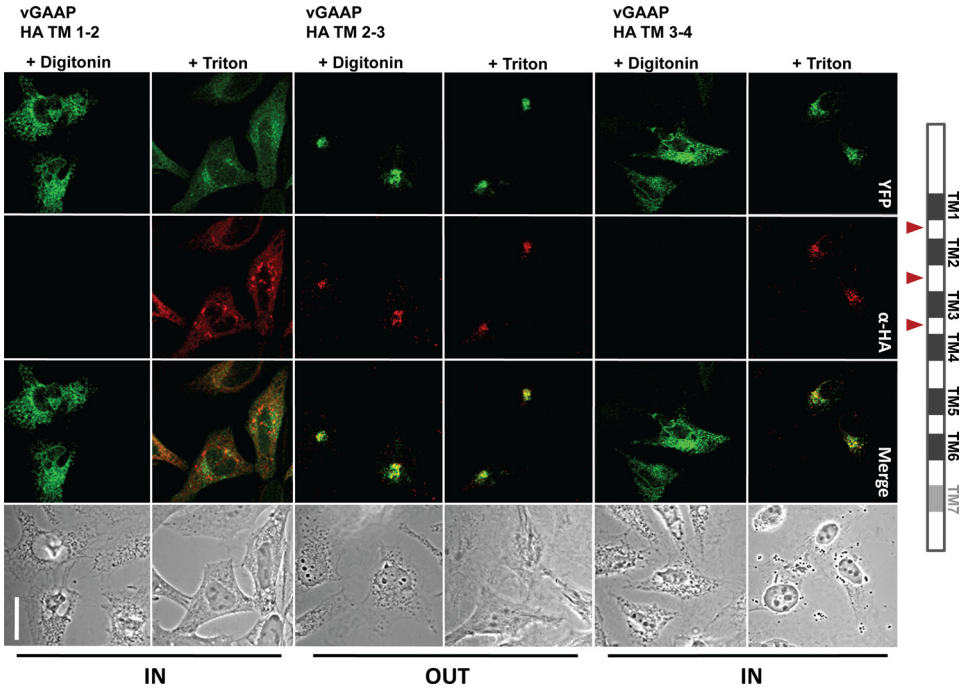

FIGURE 6. **Topology of vGAAP intermembrane loops.** HeLa cells were transfected with plasmids expressing vGAAP-YFP containing an HA tag (*red triangles*) between putative TMDs 1–2, 2–3, or 3–4. Cells were selectively permeabilized with Triton X-100 or digitonin and were probed with antibody to HA (*α-HA*). *IN* and *OUT* refer to the epitope being located on the luminal or cytoplasmic side of organelle membranes, respectively. *Scale bar*, 20 μm.

fused with green fluorescent protein (GFP) (21) were used to validate the assay (Fig. 2*A*). Following digitonin treatment, GRASP65-GFP, but not GalT-GFP, was immunostained (Fig. 2*A*), confirming the known orientation of their fluorescent tags (Fig. 2*B*) and indicating that the experimental conditions were suitable. Conversely, GFP tags were accessible for both alleles following complete permeabilization with Triton X-100. Overlapping of GFP fluorescence and antibody staining served as a control for the specificity of the antibody and the detection of allele-expressing cells (Fig. 2*A*). The efficiency of digitonin treatment in the assay was assessed by counting the percentage of cells positive (*black*) or negative (*gray*) for GFP antibody staining within the transfected cell population, which are marked by the expression of the fluorescently tagged alleles GRASP65-GFP and GalT-GFP (Fig. 2*D*). Quantification of positively *versus* negatively stained cells was also carried out for a number of chosen alleles used in this study. These include the C-terminal fluorescently tagged vGAAP, hGAAP, and BI-1

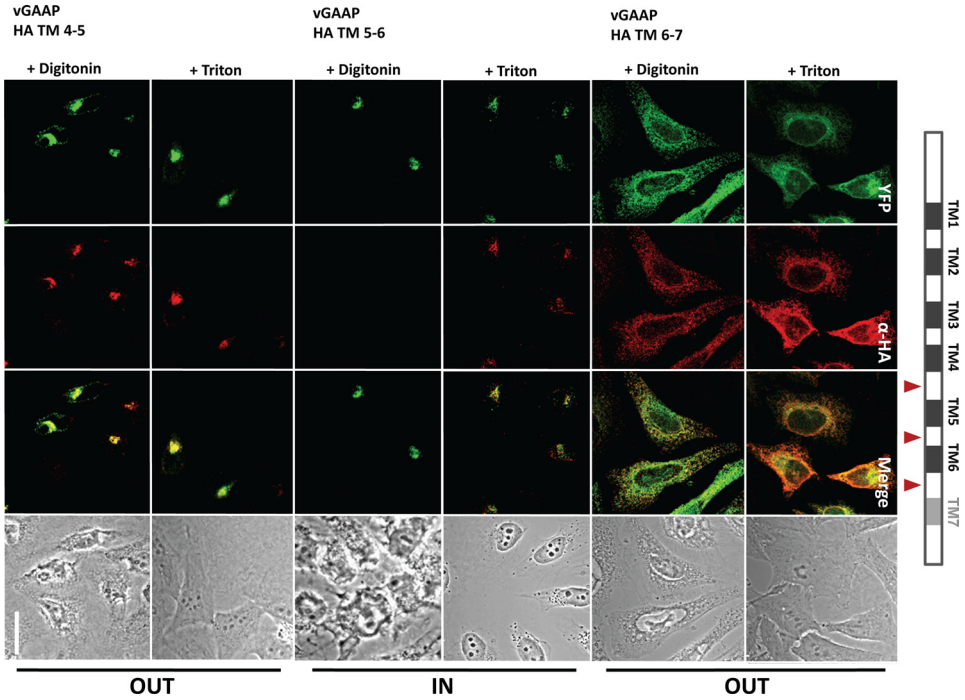

FIGURE 7. **Topology of vGAAP intermembrane loops.** HeLa cells were transfected with plasmids expressing vGAAP-YFP containing an HA tag (*red triangles*) between predicted TMDs 4–5, 5–6, or 6–7. Cells were selectively permeabilized with Triton X-100 or digitonin and were probed with HA antibody (*α-HA*). *Scale bar*, 20 μm.

alleles; the N-terminal V5-tagged hGAAP cell line; two vGAAP HA insertions of determined opposite orientations between TM 1–2 and 4–5; and the BI-1 HA insertion between TM 6–7 (supplemental Fig. 6).

N and C Termini of vGAAP, hGAAP, and BI-1 are in the Cytosol—A panel of alleles of vGAAP, hGAAP, and BI-1 was generated, and the expression as well as the expected sizes of these alleles was confirmed by immunoblotting against their respective tags or fusion proteins (Fig. 3). These alleles are vGAAP and hGAAP fused to YFP or HA at the C terminus, vGAAP fused to a V5 tag at the N terminus, BI-1 fused with CFP at the N or C terminus, and vGAAP-YFP in which an HA epitope was inserted between each pair of predicted TMDs separately. Furthermore, the expression of vGAAP-HA by transient transfection was shown to be similar to endogenous levels of vGAAP during infection (supplemental Fig. 5).

The orientations of both N and C termini were determined using a panel of N- and C-terminally tagged proteins. The N termini of vGAAP and hGAAP were first determined by immunostaining with a polyclonal antibody raised against an N-terminal peptide of GAAP (1). Following both digitonin or Triton X-100 treatment, the N termini of vGAAP and hGAAP were immunostained and therefore accessible to the antibody (Fig. 4*A*). A cell line expressing an N-terminally V5-tagged hGAAP was also used (Fig. 4*A*). Immunostaining of these tags therefore confirms bioinformatic predictions that the N termini of both vGAAP and hGAAP are located in the cytosol. The N terminus of BI-1 was detected following transient transfection of an N-terminally CFP-tagged plasmid. After permeabilization with digitonin, immunostaining with an anti-CFP antibody was successful, showing that this N terminus was also cytosolic (Fig. 4*B*). The fluorescent tag was also accessible in the complete permeabilization control with Triton X-100 (Fig. 4*B*). GAAP and BI-1 localized to the Golgi and ER, respectively, consistent with the literature (supplemental Figs. 2 and 4) (1, 10).

To determine the orientation of the C termini, C-terminally YFP- or CFP-tagged proteins were expressed and immunostained following selective or complete permeabilization of the plasma membrane. Under both conditions, all were immunostained, showing that their C termini were on the cytosolic side of the membrane (Fig. 5). This orientation was also confirmed in cells expressing C-terminally tagged vGAAP-HA (Fig. 5). Both the N and C termini of vGAAP, hGAAP, and BI-1 are therefore located in the cytoplasm.

Mapping the Orientation of vGAAP Intermembrane Loops—The cytoplasmic localization of both N and C termini precluded the previously described seven-TMD topology. However, a number of topology profiles are possible if a combination of TMDs and reentrant loops are present. To map each transmembrane region, a nine-amino acid HA tag was inserted into each of the hydrophilic loops of vGAAP individually (Fig. 1*A*, *triangles*). The orientation of the tagged regions was determined by their accessibility to HA antibody following selective or complete permeabilization of membranes. Each allele was fused to GFP at the C terminus so that fluorescence could be used as an indication of the presence of the protein.

HA tags inserted between putative TMD 1–2, 3–4, and 5–6 could not be immunostained following digitonin permeabilization, signifying that these loops are located in the Golgi lumen (Figs. 6 and 7). However, each HA tag was accessible to anti-HA following complete permeabilization of membranes with Triton X-100 (Figs. 6 and 7). Conversely, HA tags located between predicted TMD 2–3, 4–5, and 6–7 were accessible to anti-HA after both selective and complete permeabilization with digito-

nin and Triton X-100, respectively (Figs. 6 and 7), demonstrating that these loops are located on the cytosolic side of the membrane. It is of note that the HA insertion between TMD regions 1–2, 3–4, and 6–7 caused a change in localization from the Golgi to the ER, suggesting that these loops may be important for the localization of vGAAP (Figs. 6 and 7 and supplemental Fig. 3). These data allow us to propose a model for the topology of vGAAP, hGAAP, and BI-1, composed of six TMDs, with the predicted TMD 7 being either cytosolic or possibly forming a reentrant loop.

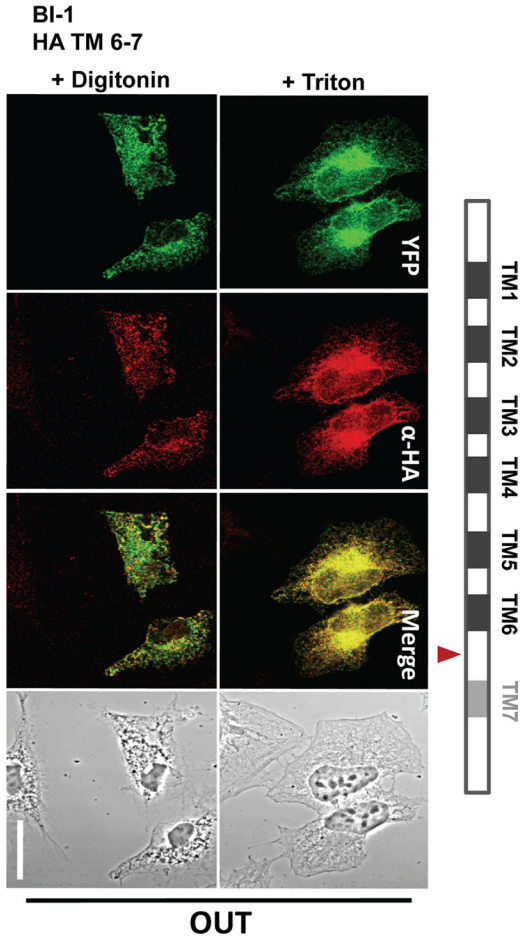

FIGURE 8. **Location of loop between BI-1 putative TMD 6 and 7.** HeLa cells were transfected with plasmids expressing BI-1-YFP containing a HA tag (*red triangle*) inserted between putative TMD 6 and 7. Cells were selectively permeabilized with Triton X-100 or digitonin, and were probed with HA antibody (α-*HA*). *Scale bar*, 20 μm.

Confirmation of Six-TMD Topology for BI-1—To determine whether BI-1 also had the six-TMD topology, the location of the loop critical for determining the presence of the predicted TMD 7 was investigated. An HA tag was inserted between putative TMD 6–7 (Fig. 1*B*). This tag was immunostained following either selective or complete permeabilization, signifying that this loop is located in the cytosol (Fig. 8). Taken together, the cytosolic location of both this loop and the C terminus confirms that, as for vGAAP, the predicted TMD 7 of BI-1 cannot span the whole membrane. Therefore, it may form a cytosolic helix or a reentrant loop and fits the proposed six-TMD topology model.

vGAAP Putative Reentrant Loop Remains Associated with Cellular Membranes—Upon permeabilization of the plasma membrane with digitonin, cytosolic membrane-free proteins are washed out, as is the case for the free YFP control, whereas membrane-spanning or associated proteins, such as full-length vGAAP-HA, remain in the cell and are detected with HA antibody (Fig. 9). The allele consisting of only vGAAP from the end of TMD 6 to the C terminus (amino acids 203–237) fused to HA was detectable after both Triton X-100 and digitonin treatment, whereas a cytosolic portion was lost in the wash (Fig. 9). This is what would be expected of a loosely membrane-associated protein and would suggest that the predicted TMD 7 of vGAAP is indeed a reentrant loop rather than a cytosolic region of the protein. However, it should be noted that it is not certain that the topology adopted by this truncated allele is that of the full-length vGAAP.

Charged Amino acids at C Terminus of hGAAP Are Required for Its Anti-apoptotic Function—Deletion or mutation of the C-terminal most 9 amino acids (EKDKKKEKK) to alanine in BI-1 from human, *Drosophila*, tomato, and yeast, have been described to be important for a number of functions including the inhibition of Bax-induced apoptosis in yeast (13, 17). In hGAAP there is also a charged series of amino acids although this is shorter (Fig. 10*A*). To assess whether these residues are important for GAAP-mediated protection against apoptosis, the C-terminal residues (LEAVNKK) were mutated to alanine (LAAVAAA) in hGAAP Cmut (Fig. 10*A*). The wild-type hGAAP and hGAAP Cmut were expressed from stable cell

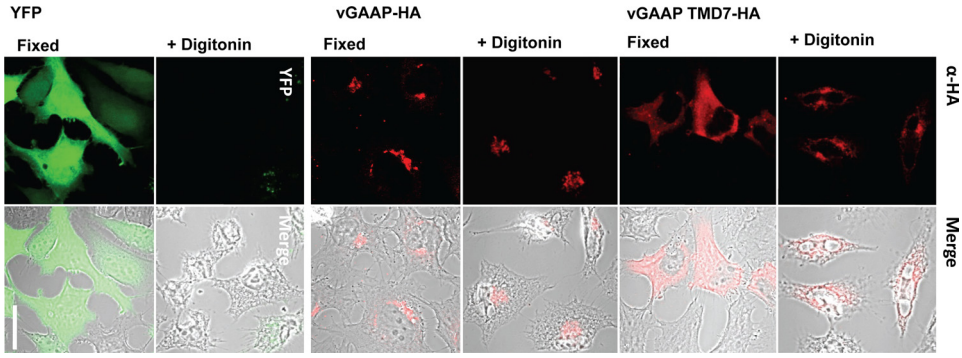

FIGURE 9. **Proposed reentrant loop remains associated with cellular membranes.** HeLa cells were transfected with plasmids expressing vGAAP-HA, vGAAP TMD 7-HA truncation, and free YFP. Cells were either fixed with paraformaldehyde and treated with 0.1% Triton X-100, or permeabilized with digitonin followed by fixation. In the latter case, membrane-free proteins were washed out, and membrane-associated proteins were probed with antibody to HA (α-*HA*). *Scale bar*, 20 μm.

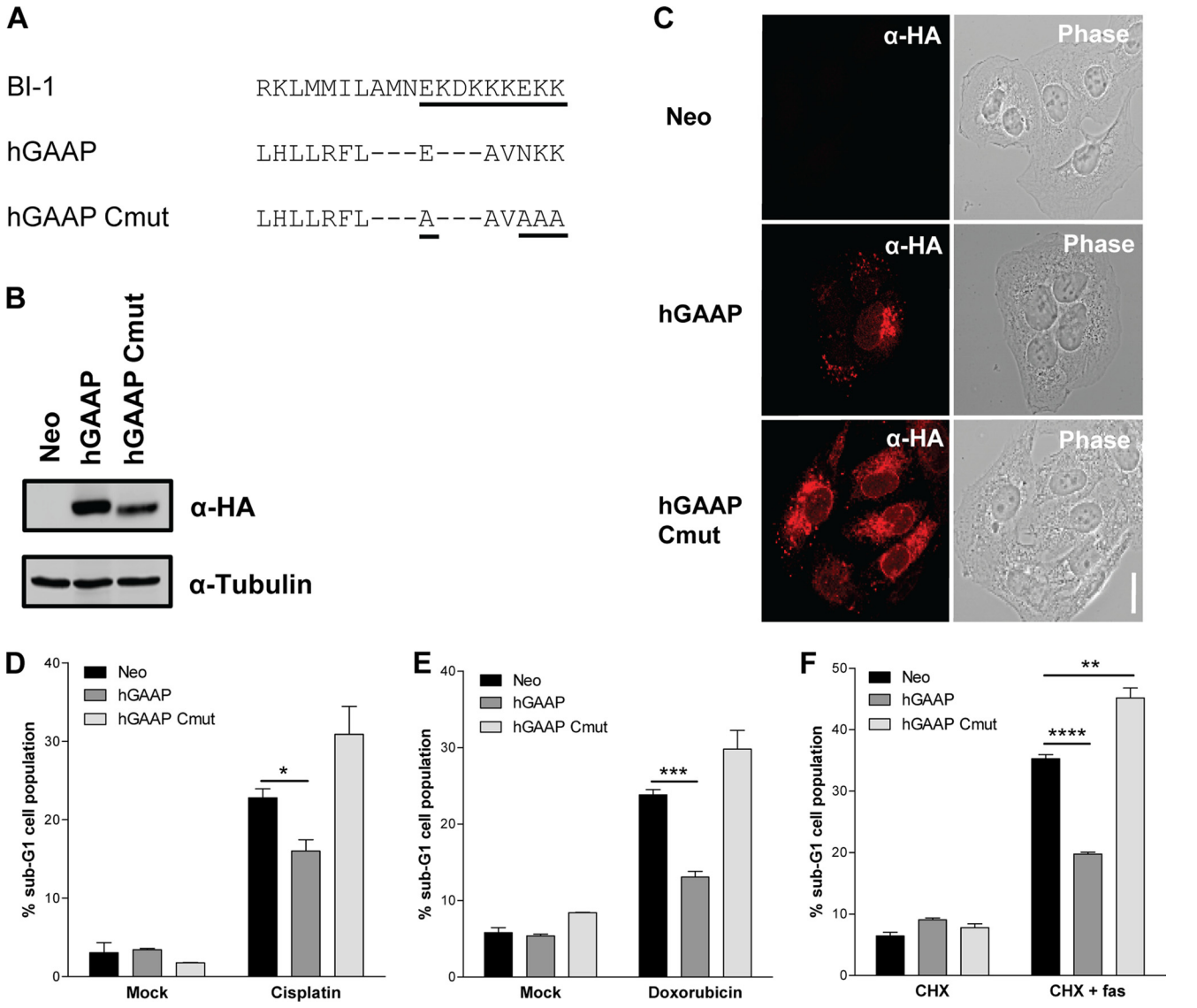

FIGURE 10. **Series of charged residues at hGAAP C terminus are required for inhibition of Fas, cisplatin, and doxorubicin-induced apoptosis.** *A*, amino acid sequence of the human BI-1 charged C terminus required for anti-apoptotic function is *underlined*. Conserved residues in the hGAAP C terminus were mutated to alanine. *B*, expression of Neo, hGAAP, and hGAAP Cmut U2OS cell lines was immunoblotted using HA antibody. *C*, confocal microscopy of Neo, hGAAP, and hGAAP Cmut U2OS cell lines probed with HA antibody is shown. *Scale bar*, 20 μm. *D–F*, Neo, hGAAP, and hGAAP Cmut U2OS cell lines were mock-treated or treated with 10 μg/ml cisplatin for 24 h (*D*), 3 μM doxorubicin for 48 h (*E*), or 10 μg/ml cycloheximide alone or together with 500 ng/ml anti-Fas antibody for 24 h (*F*). Cells were analyzed using flow cytometry. Data are presented as the mean (± S.D. (*error bars*)) percentage of sub-G_1 cells of a representative set of results from three independent experiments, each carried out in triplicate. Statistical analyses were carried out using unpaired Student's *t* test; *, $p < 0.05$; **, $p < 0.005$; ***, $p < 0.0005$; ****, $p < 0.00005$.

lines, and immunoblotting showed that proteins of the predicted sizes were present in these cells (Fig. 10*B*). The localization of hGAAP Cmut was less restricted to the Golgi compared with wild-type hGAAP (Fig. 10*C*). These cells, or control cells expressing only the selectable marker (Neo), were treated with 10 μg/ml cisplatin or 3 μM doxorubicin to test for their ability to protect cells against intrinsic pro-apoptotic stimuli. Quantification of sub-G_1 cell populations revealed that whereas hGAAP was able to reduce apoptosis significantly by 30 and 46% in cisplatin- and doxorubicin-treated cells, respectively, compared with Neo, this protection was lost in hGAAP Cmut-expressing cells (Fig. 10, *D* and *E*). To test whether these residues are also important for protection against apoptosis triggered through the extrinsic pathway, Neo, hGAAP, and hGAAP Cmut cell lines were treated with cycloheximide only or together with 500 ng/ml anti-Fas antibody. Flow cytometry showed a 44% reduction in apoptosis in wild-type hGAAP compared with Neo-expressing cells, but no protection in hGAAP Cmut cell lines (Fig. 10*F*).

The described GAAP topology model therefore maps these functionally important, conserved charged residues on the cytoplasmic side of the membrane, an orientation that is also conserved in vGAAP and BI-1 (Fig. 11).

DISCUSSION

The membrane topology of members of the TMBIM protein family has been uncertain, and both a six- and seven-TMD model has been generated depending on the bioinformatics software used. These different models place the N and C termini on either the same or opposite sides of the membrane and

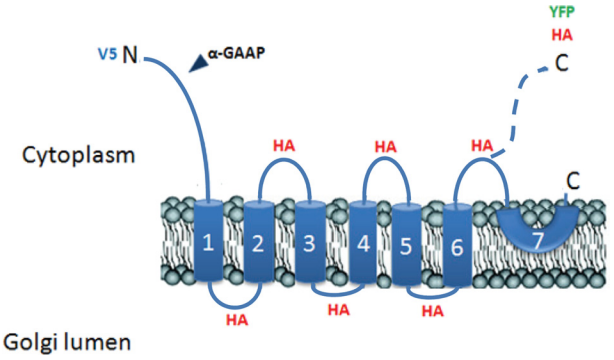

FIGURE 11. **Membrane topology model of GAAPs and BI-1.** The six-TMD model of vGAAP with a cytosolic orientation of both N and C termini is conserved in vGAAP, hGAAP, and BI-1. A putative reentrant loop (*7*) is shown with an alternative cytosolic localization (*dashed line*). The location of tags used in this study (v5, HA, YFP) which were used to demonstrate the TMDs 1–6, and the N-terminal peptide targeted by the GAAP antibody (*arrowhead*) are annotated.

consequently have important implications for interactions with other cellular proteins and for function. This study set out to determine experimentally the topology of one TMBIM family member (vGAAP) in detail and also to investigate whether this was conserved in other TMBIM members, hGAAP and BI-1. Data presented show that vGAAP has six TMDs, rather than the more commonly predicted seven TMDs, and both N and C termini are on the cytosolic side of the membrane (Fig. 11). A more limited mapping of the topology of BI-1 and hGAAP is entirely consistent with this model; and given the high conservation of amino acid sequence, length, and hydrophobicity profile of TMBIM family members (1, 3) it is very likely that this model will apply to all TMBIM members.

In vGAAP the hydrophobic helical regions are linked by short intermembrane loops ranging from 3 to 11 amino acids long, and there is a short cytosolic tail of ~35 amino acids at the N terminus. Notably, the luminal loops of vGAAP are the shortest, with about 3 amino acids between TMD 3–4 and 5–6, whereas cytosolic loops are longer with 6–7 amino acids (Figs. 1*A* and 11). This organization is also apparent for other members of the TMBIM protein family (supplemental Fig. 1). A series of hydrophobic residues toward the C terminus were predicted by some algorithms to form a seventh TMD (Fig. 1*A*). However, this prediction is incorrect because both the vGAAP C terminus and an HA tag inserted at the C terminus of TMD 6 were mapped to the cytosol. It is therefore possible that this region forms a reentrant loop (Fig. 11, *TMD7*), and the ability of the C-terminal 35 amino acids alone to remain membrane-associated upon permeabilization of the plasma membrane (Fig. 9) is consistent with this hypothesis. Alternatively, this region may form a short cytosolic tail of about 40 amino acids, similar in length to the N-terminal tail (Fig. 11, *dashed line*).

According to prediction tools, the size and length of each TMD appear to be highly conserved between members of the TMBIM family (supplemental Fig. 1); however, a further three members (GRINA/TMBIM3, Ghitm/TMBIM5, and BI-1/TMBIM6) of the six examined had disparities about the presence of the predicted seventh TMD, depending on the algorithm used. To explore the level of the conservation of GAAP topology within the family, topology mapping was extended to another member of the TMBIM family, BI-1, a protein that shares 28% identity (45% similarity) with vGAAP (1). The N and C termini of BI-1 were also in the cytosol in agreement with a recent report (18). Moreover, the vGAAP six-TMD topology was confirmed in BI-1 as the C terminus and the loop between predicted TMDs 6–7 were both mapped to the cytoplasm, thus negating the presence of a seventh complete TMD. Conservation of vGAAP topology in BI-1 is in accordance with the evolutionary theory that expansion of 5 of 7 family members (GRINA, Lfg, RESC1, GAAP, Tmbm1b), arose from a single Lfg-4-like, or GAAP-like, ancestor, which arose before the divergence of plants, and protozoa about 2,000 MYa (3). We therefore propose that the vGAAP six-TMD topology with a possible reentrant loop at the C terminus (Fig. 11) may be used as a model for BI-1 as well as other members of the TMBIM family.

The multiple helical transmembrane topology of GAAPs and BI-1 with short hydrophilic regions and a probable reentrant loop at the C terminus is reminiscent of the α-subunits of ion channels (28). If this were the case, the reentrant loop might form the pore domain or selectivity filter, although it would lack one of the two flanking transmembrane helices, which is a classical structural feature of pore-loop channels (29). However, an ion channel function has been suggested for BI-1 from a whole cell patch clamping experiment (17) and from some amino acid similarity in the proposed C-terminal reentrant loop with the loop domain of the voltage-gated sodium channel SCN5A (19). Recently, a 20-amino acid peptide corresponding to the proposed reentrant loop in BI-1 was found to be sufficient for causing a Ca^{2+} leak from the ER, and amino acid Asp-213 was found essential for this function in full-length BI-1 (18). These data therefore suggest the presence of a selectivity filter or pore domain in this region, which would fit our described C-terminal reentrant loop topology model. Such a function for BI-1 may tie in its other functions such as its ability to form oligomers, regulate Ca^{2+} concentrations in the ER and cytoplasm by rendering ER membranes more porous to Ca^{2+} (14, 15), and its mediation of Ca^{2+} efflux in BI-1 reconstituted liposomes (30). Similarly, hGAAP has also been described to regulate intracellular Ca^{2+} fluxes, lowering basal Ca^{2+} contents in intracellular stores and the release of Ca^{2+} from stores in response to inositol 1,4,5-trisphosphate (7). The described topology of BI-1 is therefore supportive of its suggested ion channel function, which may also be conserved in GAAP.

The described topology places the C-terminal cluster of charged residues from vGAAP, hGAAP, and BI-1 in the cytosol. These residues in BI-1, EKDKKKEKK, are known to be important for its anti-apoptotic function (13) and regulation of basal ER Ca^{2+} storage in a pH-dependent manner (15). Like BI-1, the equivalent C-terminal charged residues in hGAAP, EAVNKK, are important for its ability to inhibit apoptosis triggered through both intrinsic and extrinsic pathways, although the mechanism involved is not known. However, the location of this region in the cytosol is likely to be important for the mechanisms involved in mediating GAAP and BI-1 anti-apoptotic function.

Considering that the transmembrane regions make up the main component of GAAP and other TMBIM family members,

the extent of their conservation implies that structure must be important for their function. In view of the difficulties in purifying and crystallizing such hydrophobic, membrane proteins and the absence of a crystal structure for any of the members of the family, the elucidation of the topology offers an informative alternative and has implications for our understanding of the function of GAAPs, an important but poorly understood series of proteins, as well as other members of the TMBIM family.

Acknowledgments—We thank Dr. Theresa Ward, London School of Hygiene and Tropical Medicine, for plasmids GalT-GFP and GRASP65-GFP, and Rick Randall, University of St. Andrews, United Kingdom, for the HIV-1-based lentivirus system.

REFERENCES

1. Gubser, C., Bergamaschi, D., Hollinshead, M., Lu, X., van Kuppeveld, F. J., and Smith, G. L. (2007) A new inhibitor of apoptosis from Vaccinia virus and eukaryotes. *PLoS Pathog.* **3,** e17
2. Gubser, C., and Smith, G. L. (2002) The sequence of camelpox virus shows it is most closely related to Variola virus, the cause of smallpox. *J. Gen. Virol.* **83,** 855–872
3. Hu, L., Smith, T. F., and Goldberger, G. (2009) LFG: a candidate apoptosis regulatory gene family. *Apoptosis* **14,** 1255–1265
4. Alcamí, A., and Smith, G. L. (1995) Vaccinia, cowpox, and camelpox viruses encode soluble γ-interferon receptors with novel broad species specificity. *J. Virol.* **69,** 4633–4639
5. Nuara, A. A., Walter, L. J., Logsdon, N. J., Yoon, S. I., Jones, B. C., Schriewer, J. M., Buller, R. M., and Walter, M. R. (2008) Structure and mechanism of IFN-γ antagonism by an orthopoxvirus IFN-γ-binding protein. *Proc. Natl. Acad. Sci. U.S.A.* **105,** 1861–1866
6. Lee, S., Jo, M., Lee, J., Koh, S. S., and Kim, S. (2007) Identification of novel universal housekeeping genes by statistical analysis of microarray data. *J. Biochem. Mol. Biol.* **40,** 226–231
7. de Mattia, F., Gubser, C., van Dommelen, M. M., Visch, H. J., Distelmaier, F., Postigo, A., Luyten, T., Parys, J. B., de Smedt, H., Smith, G. L., Willems, P. H., and van Kuppeveld, F. J. (2009) Human Golgi antiapoptotic protein modulates intracellular calcium fluxes. *Mol. Biol. Cell* **20,** 3638–3645
8. Walter, L., Marynen, P., Szpirer, J., Levan, G., and Günther, E. (1995) Identification of a novel conserved human gene, TEGT. *Genomics* **28,** 301–304
9. Somia, N. V., Schmitt, M. J., Vetter, D. E., Van Antwerp, D., Heinemann, S. F., and Verma, I. M. (1999) LFG: an anti-apoptotic gene that provides protection from Fas-mediated cell death. *Proc. Natl. Acad. Sci. U.S.A.* **96,** 12667–12672
10. Xu, Q., and Reed, J. C. (1998) Bax inhibitor-1, a mammalian apoptosis suppressor identified by functional screening in yeast. *Mol. Cell* **1,** 337–346
11. Zhou, J., Zhu, T., Hu, C., Li, H., Chen, G., Xu, G., Wang, S., Zhou, J., and Ma, D. (2008) Comparative genomics and function analysis on BI1 family. *Comput. Biol. Chem.* **32,** 159–162
12. Bolduc, N., Ouellet, M., Pitre, F., and Brisson, L. (2003) Molecular characterization of two plant BI-1 homologues which suppress Bax-induced apoptosis in human 293 cells. *Planta* **216,** 377–386
13. Chae, H. J., Ke, N., Kim, H. R., Chen, S., Godzik, A., Dickman, M., and Reed, J. C. (2003) Evolutionarily conserved cytoprotection provided by Bax Inhibitor-1 homologs from animals, plants, and yeast. *Gene* **323,** 101–113
14. Xu, C., Xu, W., Palmer, A. E., and Reed, J. C. (2008) BI-1 regulates endoplasmic reticulum Ca^{2+} homeostasis downstream of Bcl-2 family proteins. *J. Biol. Chem.* **283,** 11477–11484
15. Kim, H. R., Lee, G. H., Ha, K. C., Ahn, T., Moon, J. Y., Lee, B. J., Cho, S. G., Kim, S., Seo, Y. R., Shin, Y. J., Chae, S. W., Reed, J. C., and Chae, H. J. (2008) Bax inhibitor-1 is a pH-dependent regulator of Ca^{2+} channel activity in the endoplasmic reticulum. *J. Biol. Chem.* **283,** 15946–15955
16. Cebulski, J., Malouin, J., Pinches, N., Cascio, V., and Austriaco, N. (2011) Yeast Bax inhibitor, Bxi1p, is an ER-localized protein that links the unfolded protein response and programmed cell death in *Saccharomyces cerevisiae*. *PLoS ONE* **6,** e20882
17. Lee, G. H., Ahn, T., Kim, D. S., Park, S. J., Lee, Y. C., Yoo, W. H., Jung, S. J., Yang, J. S., Kim, S., Muhlrad, A., Chae, S. W., Kim, H. R., and Chae, H. J. (2010) Bax inhibitor 1 increases cell adhesion through actin polymerization: involvement of calcium and actin binding. *Mol. Cell. Biol.* **30,** 1800–1813
18. Bultynck, G., Kiviluoto, S., Henke, N., Ivanova, H., Schneider, L., Rybalchenko, V., Luyten, T., Nuyts, K., De Borggraeve, W., Bezprozvanny, I., Parys, J. B., De Smedt, H., Missiaen, L., and Methner, A. (2012) The C terminus of Bax inhibitor-1 forms a Ca^{2+}-permeable channel pore. *J. Biol. Chem.* **287,** 2544–2557
19. Henke, N., Lisak, D. A., Schneider, L., Habicht, J., Pergande, M., and Methner, A. (2011) The ancient cell death suppressor BAX inhibitor-1. *Cell Calcium* **50,** 251–260
20. Demaison, C., Parsley, K., Brouns, G., Scherr, M., Battmer, K., Kinnon, C., Grez, M., and Thrasher, A. J. (2002) High-level transduction and gene expression in hematopoietic repopulating cells using a human immunodeficiency [correction of imunodeficiency] virus type 1-based lentiviral vector containing an internal spleen focus forming virus promoter. *Hum. Gene Ther.* **13,** 803–813
21. Ward, T. H., Polishchuk, R. S., Caplan, S., Hirschberg, K., and Lippincott-Schwartz, J. (2001) Maintenance of Golgi structure and function depends on the integrity of ER export. *J. Cell Biol.* **155,** 557–570
22. Lorenz, H., Hailey, D. W., Wunder, C., and Lippincott-Schwartz, J. (2006) The fluorescence protease protection (FPP) assay to determine protein localization and membrane topology. *Nat. Protoc.* **1,** 276–279
23. Claros, M. G., and von Heijne, G. (1994) TopPred II: an improved software for membrane protein structure predictions. *Comput. Appl. Biosci.* **10,** 685–686
24. Hirokawa, T., Boon-Chieng, S., and Mitaku, S. (1998) SOSUI: classification and secondary structure prediction system for membrane proteins. *Bioinformatics* **14,** 378–379
25. Krogh, A., Larsson, B., von Heijne, G., and Sonnhammer, E. L. (2001) Predicting transmembrane protein topology with a hidden Markov model: application to complete genomes. *J. Mol. Biol.* **305,** 567–580
26. Nugent, T., and Jones, D. (2009) Transmembrane protein topology prediction using support vector machines. *BMC Bioinformatics* **10,** 159
27. Jones, D. T. (2007) Improving the accuracy of transmembrane protein topology prediction using evolutionary information. *Bioinformatics* **23,** 538–544
28. Yu, F. H., Yarov-Yarovoy, V., Gutman, G. A., and Catterall, W. A. (2005) Overview of molecular relationships in the voltage-gated ion channel superfamily. *Pharmacol. Rev.* **57,** 387–395
29. Zhorov, B. S., and Tikhonov, D. B. (2004) Potassium, sodium, calcium and glutamate-gated channels: pore architecture and ligand action. *J. Neurochem.* **88,** 782–799
30. Ahn, T., Yun, C. H., Chae, H. Z., Kim, H. R., and Chae, H. J. (2009) Ca^{2+}/H^{+} antiporter-like activity of human recombinant Bax inhibitor-1 reconstituted into liposomes. *FEBS J.* **276,** 2285–2291